

involve

a journal of mathematics

Loewner deformations driven by
the Weierstrass function

Joan Lind and Jessica Robins



Loewner deformations driven by the Weierstrass function

Joan Lind and Jessica Robins

(Communicated by Michael Dorff)

The Loewner differential equation provides a way of encoding growing families of sets into continuous real-valued functions. Most famously, Schramm–Loewner evolution (SLE) consists of the growing random families of sets that are encoded via the Loewner equation by a multiple of Brownian motion. The purpose of this paper is to study the families of sets encoded by a multiple of the Weierstrass function, which is a deterministic analog of Brownian motion. We prove that there is a phase transition in this setting, just as there is in the SLE setting.

| | |
|-----------------------------------|-----|
| 1. Introduction and results | 151 |
| 2. A look at the Loewner equation | 154 |
| 3. The Weierstrass function | 159 |
| 4. Proof of the phase transition | 163 |
| Acknowledgement | 164 |
| References | 164 |

1. Introduction and results

Charles Loewner introduced his namesake differential equation in 1923, and the equation subsequently became an important and long-standing tool in complex analysis. Many decades later Oded Schramm rediscovered the Loewner equation as he was working on seemingly unrelated problems in probability and statistical physics. In 2000, Schramm introduced a family of random curves, which he called stochastic Loewner evolution, or SLE for short (and which have subsequently been renamed Schramm–Loewner evolution in Schramm’s honor).

Roughly speaking, the Loewner equation provides a correspondence between 2-dimensional curves and continuous 1-dimensional functions (and a more careful description will be given in the next section). Schramm discovered that the SLE

MSC2010: 30C35.

Keywords: Loewner evolution, Weierstrass function.

Lind was supported in part by NSF grant DMS-1100714.

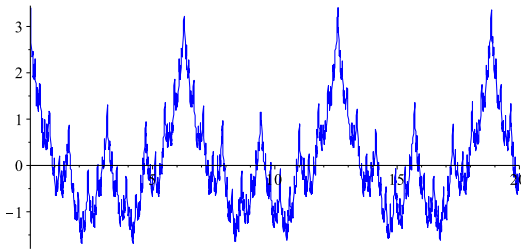


Figure 1. The Weierstrass function $W(t)$.

curves (the random 2-dimensional curves that he wanted to study) corresponded via the Loewner equation to a multiple of a well-known and much-loved random 1-dimensional function: Brownian motion. Thus, properties of Brownian motion could be leveraged to understand the SLE curves. Schramm’s revolutionary work led not only to deep results in probability and theoretical physics, but it also inspired a renewed study of the Loewner equation. There has been particular interest in how geometric properties of the 2-dimensional curves may be encoded into the corresponding 1-dimensional functions.

SLE is often written SLE_κ to emphasize that it is an infinite family of random curves depending on a parameter $\kappa \geq 0$. In particular, under the Loewner correspondence, SLE_κ corresponds to the continuous function $\sqrt{\kappa}B(t)$, where $B(t)$ is Brownian motion. The SLE_κ curves come in three flavors, depending on the value of κ : when $\kappa \in [0, 4]$, then SLE_κ is a simple curve, when $\kappa \in (4, 8)$, then SLE_κ is a curve that hits back on itself, and when $\kappa \in [8, \infty)$, then SLE_κ is a space-filling curve [Rohde and Schramm 2005]. Thus there are three geometric phases, with sharp phase transitions at $\kappa = 4$ and $\kappa = 8$. See Figure 4, which illustrates the first two phases.

In this work we look at a deterministic analog of Brownian motion, the Weierstrass function, which, like Brownian motion, is continuous but nowhere-differentiable. In particular, we work with

$$W(t) = \sum_{n=0}^{\infty} 2^{-n/2} \cos(2^n t),$$

which is graphed in Figure 1. In comparison with SLE_κ , we seek to understand the 2-dimensional sets that correspond with a multiple of the Weierstrass function via the Loewner equation. We call this family of sets “the deformations driven by the Weierstrass function”, and our main theorem establishes the existence of at least one phase transition, just as in the SLE setting. This transition from simple curve to nonsimple curve is illustrated in Figure 2, where we show approximations to the deformations driven by the Weierstrass function.

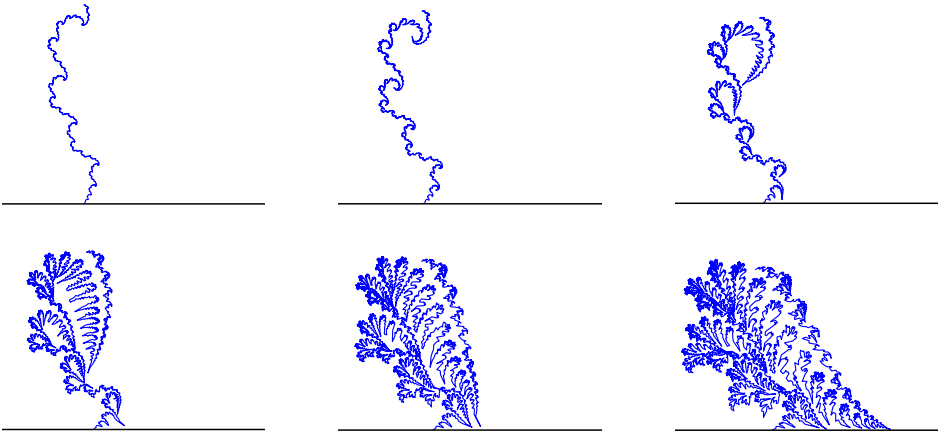


Figure 2. Simulations of the hulls generated by $cW(t)$ for $c = 0.8$ (top left), $c = 1$ (top middle), $c = 1.2$ (top right), $c = 1.4$ (bottom left), $c = 1.6$ (bottom middle), and $c = 1.8$ (bottom right).

Theorem 1.1. *The deformations driven by the Weierstrass function $W(t)$ exhibit a phase transition. In particular, when c is small enough, the hull generated by $cW(t)$ is a simple curve in $\mathbb{H} \cup \{cW(0)\}$, and this is not the case when c is large enough.*

In order to prove [Theorem 1.1](#), we will need the following result, which gives a lower bound on the growth of the Weierstrass function near its local maxima.

Theorem 1.2. *Let $t_{m,k} = m\pi/2^k$ for $m, k \in \mathbb{N}$. If $0 < |h| \leq 2^{-(k+7)}$, then*

$$W(t_{m,k}) - W(t_{m,k} + h) \geq 0.2\sqrt{|h|}.$$

This result implies that $W(t)$ has local maxima at the points $2^{-k}m\pi$. These times $2^{-k}m\pi$, which will feature in our proof of [Theorem 1.1](#), correspond to the rightward-pointing “beaks” seen in the curves of [Figure 2](#). One difference between Brownian motion and the Weierstrass function is that Brownian motion behaves similarly at its local maximums and local minimums, while the Weierstrass function favors its local maximums (that is, there is greater increase as one moves towards the local maximums than there is decrease moving towards the local minimums). This is also visually discernible in [Figure 2](#) in the fact that there are obvious “beaks” to the right but not to the left.

Although we chose to focus on the Weierstrass function in this paper, we wish to note that our approach applies more generally. In fact, any $\text{Lip}(\frac{1}{2})$ function that has the behavior shown in [Theorem 1.2](#) will exhibit a phase transition.

This paper is organized as follows. We discuss the Loewner equation in [Section 2](#), with a focus on the particular aspects of the Loewner theory that will be needed

to prove [Theorem 1.1](#). [Section 3](#) regards the Weierstrass function and contains the proof of [Theorem 1.2](#). In [Section 4](#) we bring the Weierstrass function and the Loewner equation together to prove [Theorem 1.1](#).

2. A look at the Loewner equation

In this section, we introduce the Loewner equation, consider some examples, and discuss the features of the Loewner equation that will be relevant for our work. We refer interested readers to the survey article [[Gruzberg and Kadanoff 2004](#)] and the references therein for more information about the Loewner equation and SLE.

Background and examples. The Loewner equation gives a correspondence between continuous, real-valued functions and certain growing families of sets in the complex plane. Given a function, we will describe how to obtain the family of sets via the Loewner equation. To that end, let λ be a continuous, real-valued function defined on $[0, T]$, and choose an initial point $z_0 \in \overline{\mathbb{H}} \setminus \{\lambda(0)\}$, where $\mathbb{H} = \{x + iy : y > 0\}$ denotes the upper half-plane. Then the chordal Loewner differential equation is the initial value problem

$$\frac{d}{dt}z(t) = \frac{2}{z(t) - \lambda(t)}, \quad z(0) = z_0. \quad (2-1)$$

A unique solution $z(t)$ exists on some time interval, by the existence and uniqueness theorem for differential equations. In fact, the solution $z(t)$ will continue to exist unless the denominator in (2-1) is zero, which occurs if $z(s) = \lambda(s)$ for some s . When this happens, we say that z_0 is captured by λ at time s . We define the hull at time t , notated K_t , to be the collection of captured points:

$$K_t = \{z_0 \in \overline{\mathbb{H}} : z(s) = \lambda(s) \text{ for some } s \leq t\}.$$

This family of hulls, $\{K_t\}_{t \in [0, T]}$, is the increasing family of sets that correspond to $\lambda(t)$ via the Loewner equation. We call λ the driving function, and we say that K_t is generated by λ .

We wish to take a moment to discuss the Loewner equation further in an informal manner. To begin, think of watching the movement of two particles in the plane. One particle moves only on \mathbb{R} (and its position is given by $\lambda(t)$), and the other particle (described by $z(t)$) moves in $\overline{\mathbb{H}}$ but its movement is controlled by its relationship to the first particle via (2-1). To put a little action into our story, we think of the second particle as trying to escape from the first, while the first is trying to capture the second. To justify this storyline, let's suppose that $z_0 \in \mathbb{R}$, in which case both particles are moving along \mathbb{R} . Then (2-1) implies that the particle described by $z(t)$ is always moving away from the other particle (i.e., "trying to escape"). As we will



Figure 3. The hulls K_1 generated by $c - c\sqrt{1-t}$ for $c = 3$ (left) and $c = 5$ (right).

see later, if the particle described by $\lambda(t)$ moves quickly enough, it can catch up to the second particle and “capture” it (meaning that $\lambda(s) = z(s)$ at some time s).

We will briefly discuss some examples (and we refer the reader to [Kager et al. 2004] for the detailed analysis of these examples).

Example 1. When $\lambda(t) \equiv 0$, then $K_t = \{iy : 0 \leq y \leq 2\sqrt{t}\}$, a growing vertical line segment. To see why this might be true, we decompose (2-1) with $\lambda(t) \equiv 0$ into its real and imaginary parts:

$$\frac{d}{dt} \operatorname{Re}(z(t)) = \frac{2 \operatorname{Re}(z(t))}{|z(t)|^2} \quad \text{and} \quad \frac{d}{dt} \operatorname{Im}(z(t)) = -\frac{2 \operatorname{Im}(z(t))}{|z(t)|^2}.$$

This implies that $\operatorname{Im}(z(t))$ is decreasing, and $\operatorname{Re}(z(t))$ is increasing when $\operatorname{Re}(z_0) > 0$ and decreasing when $\operatorname{Re}(z_0) < 0$. In other words, points to the right of λ stay to the right, and points to the left of λ stay to the left. Thus the only possible points that could be captured by λ are those along the imaginary axis, since these points follow a downward trajectory toward λ .

Example 2. When $\lambda(t) = c\sqrt{t}$, then K_t is a growing line segment, beginning at 0. The angle between the line segment and \mathbb{R} depends on c . This example is not as easy to justify as the first. One could either derive this result computationally (as done in [Kager et al. 2004]) or one could justify it using a scaling property of the Loewner equation. Neither approach, however, is relevant to the work in our paper, and we omit it.

In the first two examples, the hulls are growing simple curves in $\mathbb{H} \cup \{\lambda(0)\}$, by which we mean that there exists a simple curve $\gamma : [0, T] \rightarrow \mathbb{H} \cup \{\lambda(0)\}$ so that $K_t = \gamma([0, t])$. Initially, one might wonder if this is always true. The next example, however, shows us otherwise.

Example 3. Let $\lambda(t) = c - c\sqrt{1-t}$. For $0 < c < 4$, the hulls K_t are simple curves for all $t \in [0, 1]$. When $c \geq 4$, the same is true for the initial hulls; that is, for $t < 1$, K_t are simple curves. At $t = 1$, however, the geometry of the situation changes. Here the simple curve hits back on \mathbb{R} , and forms a “bubble”, and so the final hull K_1 contains the curve, the points in \mathbb{H} under the curve, and an interval from \mathbb{R} . See Figure 3.

Examples 2 and 3 each contain a family of examples, which we call a family of deformations. Our precise definition follows:

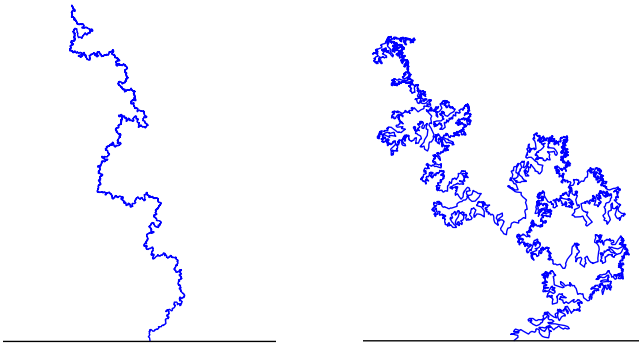


Figure 4. Simulations of an SLE_2 hull (the curve on the left) and an SLE_6 hull (the curve on the right together with all the bubbles formed).

Definition. Let λ be a continuous function defined on $[0, T]$. The family of deformations driven by λ is the family of hulls K_T^c generated by $c\lambda$ for $c > 0$.

Examples 2 and 3 gave the family of deformations driven by \sqrt{t} and $1 - \sqrt{1 - t}$. In Example 2, the hulls are simple curves for all values of c . However, there is a phase transition in Example 3: the hulls are simple curves for small c , but this fails to be the case for large c . Although this family is already well understood, we will prove the existence of this phase transition in Corollary 2.4 as an illustration of our method.

Example 4. SLE_κ , the best known example of a family of deformations, consists of the random hulls generated by $\sqrt{\kappa}B(t)$, where $B(t)$ is Brownian motion. As mentioned in the introduction, this family does exhibit phase transitions [Rohde and Schramm 2005]. In particular, when $\kappa \leq 4$, the hulls are simple curves (as illustrated in the left-hand picture of Figure 4), but this fails to be the case for $\kappa > 4$. When $4 < \kappa < 8$, the SLE_κ hull is the union of a random curve together with all the bubbles that are formed when the curve hits back on itself or on the real line (see the right-hand picture of Figure 4.) When $\kappa \geq 8$, there is a second phase transition, and the hulls become space-filling curves.

Criteria for hull behavior. In order to show that a family of deformations has a phase transition, we will need to be able to determine whether or not a hull is a simple curve, based on some feature of the driving function. In particular, our goal is to find two criteria; the first one (Theorem 2.1) will guarantee a simple-curve hull, and a second one (Proposition 2.2) will imply a nonsimple-curve hull. As an example, we will apply both of these to the driving function $c - c\sqrt{1 - t}$ to verify the phase transition that we have discussed (see Corollary 2.4).

To formulate the first criterion, we need to define what it means for a function to be $\text{Lip}(\frac{1}{2})$, also known as Hölder continuous with exponent $\frac{1}{2}$.

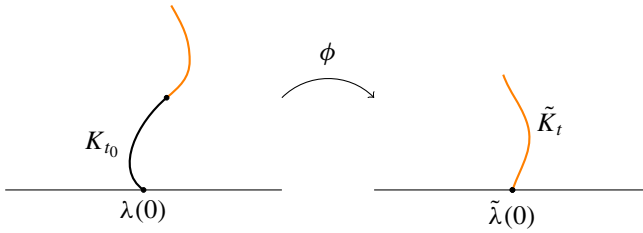


Figure 5. An illustration of the concatenation property.

Definition. A function $\lambda(t)$ defined on an interval $[0, T]$ is said to be a $\text{Lip}(\frac{1}{2})$ function if there exists some $M < \infty$ so that

$$|\lambda(t) - \lambda(s)| \leq M\sqrt{|t - s|}$$

for all $t, s \in [0, T]$. The smallest such M for which this holds is called the $\text{Lip}(\frac{1}{2})$ norm of λ , notated $\|\lambda\|_{1/2}$.

Examples of $\text{Lip}(\frac{1}{2})$ functions include $c\sqrt{t}$ and $c - c\sqrt{1-t}$, both of which have $\text{Lip}(\frac{1}{2})$ norm $|c|$. Further, any differentiable function will also be a $\text{Lip}(\frac{1}{2})$ function. If $\lambda(t)$ is a $\text{Lip}(\frac{1}{2})$ function with norm M , then $c\lambda(t)$ is also a $\text{Lip}(\frac{1}{2})$ function and $\|c\lambda\|_{1/2} = |c|M$.

We use the following criterion when we want to guarantee we have a simple curve.

Theorem 2.1 [Lind 2005, Theorem 2]. *If λ is a $\text{Lip}(\frac{1}{2})$ function with $\|\lambda\|_{1/2} < 4$, then the hulls generated by λ are all simple curves contained in $\mathbb{H} \cup \{\lambda(0)\}$.*

Next, we wish to formulate a criterion that will imply that a particular hull is not a simple curve. Consider [Example 3](#), where the driving function is $c - c\sqrt{1-t}$. If we compare the final hulls generated when $c = 3$ and when $c = 5$, we notice one key difference: the latter hull contains an interval along the real line, whereas the former contains no real-valued points except for the initial point. This means that in the second situation, there exists a real-valued point that is captured by λ at time 1. This observation, combined with the following property of the Loewner equation, leads to our second criterion, [Proposition 2.2](#) below.

Concatenation property of the Loewner equation. Let λ be a continuous function defined on $[0, T]$ and let K_t be the hulls generated by λ . For $t_0 \in (0, T)$, let \tilde{K}_t be the hulls generated by the time-shifted driving function $\tilde{\lambda}(t) = \lambda(t_0 + t)$ for $t \in [0, T - t_0]$. Then $\tilde{K}_t = \phi(K_{t_0+t} \setminus K_{t_0})$, where ϕ is the unique conformal map from $\mathbb{H} \setminus K_{t_0}$ onto \mathbb{H} with the following normalization at infinity: $\phi(z) = z + O(1/z)$.

Note that a conformal map between two domains is a homeomorphism that is also complex differentiable. The concatenation property is illustrated in [Figure 5](#). Here the black curve is K_{t_0} , and ϕ is a conformal map from $\mathbb{H} \setminus K_{t_0}$ (that is, \mathbb{H}

with the black curve removed) onto \mathbb{H} . The orange curve on the left represents $K_{t_0+t} \setminus K_{t_0}$, and the image of this set under ϕ is the orange curve on the right.

Proposition 2.2. *Let λ be a continuous function defined on $[0, T]$. Suppose there exists some $t_0 \in [0, T)$ and some $s \in (0, T - t_0]$ so that the time-shifted driving function $\tilde{\lambda}(t) = \lambda(t_0 + t)$ captures a real-valued point at time s . Then the hull K_{t_0+s} generated by λ is not a simple curve contained in $\mathbb{H} \cup \{\lambda(0)\}$.*

Proof. Since $\tilde{\lambda}(t)$ captures a real-valued point at time s , the corresponding hull \tilde{K}_s must contain at least one point in \mathbb{R} that is not the initial point $\tilde{\lambda}(0)$. But this implies that \tilde{K}_s cannot be a simple curve in $\mathbb{H} \cup \{\tilde{\lambda}(0)\}$.

If K_{t_0+s} is a simple curve in $\mathbb{H} \cup \{\lambda(0)\}$, then $K_{t_0+s} \setminus K_{t_0}$ must be a simple curve in $\mathbb{H} \setminus K_{t_0}$. The concatenation property implies that \tilde{K}_s is the image of $K_{t_0+s} \setminus K_{t_0}$ under a homeomorphism taking $\mathbb{H} \setminus K_{t_0}$ to \mathbb{H} , and so \tilde{K}_t must also be a simple curve in $\mathbb{H} \cup \{\tilde{\lambda}(0)\}$. Since this is not the case, K_{t_0+s} cannot be a simple curve in $\mathbb{H} \cup \{\lambda(0)\}$. □

As an example, we wish to apply [Theorem 2.1](#) and [Proposition 2.2](#) to the hulls generated by $c - c\sqrt{1-t}$ to prove that this family has a phase transition. The following lemma, which we will use again later, provides part of the argument.

Lemma 2.3. *Let $c \geq 4$, $\tau > 0$, and $a \in \mathbb{R}$, and set $b = \frac{1}{2}(-c + \sqrt{c^2 - 16})$. Then $x(t) = a + b\sqrt{\tau - t}$ is a solution to (2-1) when $\lambda(t) = a - c\sqrt{\tau - t}$. In particular, the driving function $a - c\sqrt{\tau - t}$ captures a real-valued point at time τ .*

Proof. To show the first statement, we must simply verify that

$$x'(t) = \frac{2}{x(t) - \lambda(t)}. \tag{2-2}$$

The left-hand side of (2-2) is $x'(t) = -b/(2\sqrt{\tau - t})$, and the right-hand side is

$$\frac{2}{(a + b\sqrt{\tau - t}) - (a - c\sqrt{\tau - t})} = \frac{2}{(b + c)\sqrt{\tau - t}}.$$

Thus (2-2) holds as long as $-b/2 = 2/(b + c)$, which can be easily verified.

The second statement follows from the fact that $x(\tau) = a = \lambda(\tau)$. □

Now [Theorem 2.1](#) and [Proposition 2.2](#) imply the following:

Corollary 2.4. *The deformations driven by $1 - \sqrt{1-t}$ exhibit a phase transition. In particular, the hull K_1^c generated by $c - c\sqrt{1-t}$ is a simple curve in $\mathbb{H} \setminus \{0\}$ when $0 \leq c < 4$, and this is not the case when $c \geq 4$.*

Proof. Since $c - c\sqrt{1-t}$ is a $\text{Lip}(\frac{1}{2})$ function with norm c , [Theorem 2.1](#) implies that K_1^c is a simple curve in $\mathbb{H} \setminus \{0\}$ when $0 \leq c < 4$.

Now suppose that $c \geq 4$. Then [Lemma 2.3](#) implies that $c - c\sqrt{1-t}$ captures a real-valued point at time 1. Thus, applying [Proposition 2.2](#) with $t_0 = 0$ and $s = 1$ gives that K_1^c is not a simple curve in $\mathbb{H} \setminus \{0\}$. □

3. The Weierstrass function

Karl Weierstrass introduced the Weierstrass function in 1872,¹ giving the first published example of a continuous function that is nowhere differentiable. The function can be written as

$$F_{a,b}(t) = \sum_{n=0}^{\infty} a^n \cos(b^n t),$$

depending on two parameters $a \in (0, 1)$ and $b \geq 1/a$.² In this paper we will work with $b = 2$ and $a = 1/\sqrt{2}$, and so we define

$$W(t) = \sum_{n=0}^{\infty} 2^{-n/2} \cos(2^n t),$$

which is graphed in [Figure 1](#). With this choice of parameters, G. H. Hardy [1916, Theorem 1.33] proved that $W(t)$ is a $\text{Lip}(\frac{1}{2})$ function. We will give a proof of Hardy’s result that allows us to calculate the following upper bound on the $\text{Lip}(\frac{1}{2})$ norm of $W(t)$.

Proposition 3.1. *The $\text{Lip}(\frac{1}{2})$ norm of $W(t) = \sum_{n=0}^{\infty} 2^{-n/2} \cos(2^n t)$ satisfies*

$$\|W\|_{1/2} \leq 12.$$

This result complements [Theorem 1.2](#), which gives a lower bound for a local version of the $\text{Lip}(\frac{1}{2})$ norm. The two results are illustrated in [Figures 6 and 7](#), where we have plotted

$$\frac{W(t_{m,k}) - W(t_{m,k} + h)}{\sqrt{|h|}}$$

as a function of h for two choices of $t_{m,k} = 2^{-k}m\pi$. The left-hand picture for each figure shows $h \in [-1, 1]$ while the right-hand image is a “zoomed-in” picture with $h \in [-0.0001, 0.0001]$. We wish to point out a few features of these pictures. First, notice that the output values have an upper bound that is unaffected by the zooming. The existence of this global upper bound is a result of the bound on the $\text{Lip}(\frac{1}{2})$ norm in [Proposition 3.1](#). A more interesting feature is the fact that the output values in the zoomed-in picture fall in a band that is bounded below. [Theorem 1.2](#) guarantees that this lower bound exists for any $t_{m,k} = 2^{-k}m\pi$, once we zoom in far enough.

The bounds we obtain in [Theorem 1.2](#) and [Proposition 3.1](#) are far from optimal when compared with our experimental data. This is evident in the right-hand

¹Weierstrass introduced his namesake function in a presentation on July 18, 1872, but his published work regarding this function [[Weierstrass 1895](#)] appeared later.

²These particular parameter values are due to Hardy [[1916](#)]; Weierstrass originally had more restrictions on the parameters.

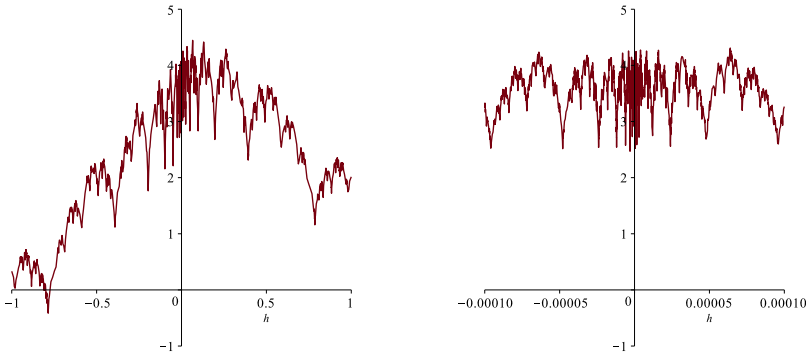


Figure 6. The graph of $(W(\pi/2) - W(\pi/2 + h))/\sqrt{|h|}$ for $h \in [-1, 1]$ (left) and for $h \in [-0.0001, 0.0001]$ (right).

pictures of Figures 6 and 7, which appear to be contained in a band between 2 and 5, a much more restrictive interval than the bounds we obtain of 0.2 and 12. The trade-off for our imprecision, however, is that our proofs are fairly straightforward.

Proof of Proposition 3.1. Set $a = 1/\sqrt{2}$. Note that

$$|W(t+h) - W(t)| \leq 2 \max_{s \in \mathbb{R}} |W(s)| = 2 \sum_{n=0}^{\infty} a^n = \frac{2}{1-a} \approx 6.8.$$

Therefore, when $|h| \geq 1$, we certainly have that $|W(t+h) - W(t)| \leq 12\sqrt{|h|}$.

For the rest of the proof, assume $0 < |h| < 1$. The trigonometric identity $\cos(x) - \cos(y) = -2 \sin(\frac{1}{2}(x+y)) \sin(\frac{1}{2}(x-y))$ implies that

$$|W(t+h) - W(t)| \leq 2 \sum_{n=0}^{\infty} a^n \left| \sin\left(\frac{1}{2} 2^n (2t+h)\right) \right| \left| \sin\left(\frac{1}{2} 2^n h\right) \right| \leq 2 \sum_{n=0}^{\infty} a^n \left| \sin(2^{n-1} h) \right|.$$

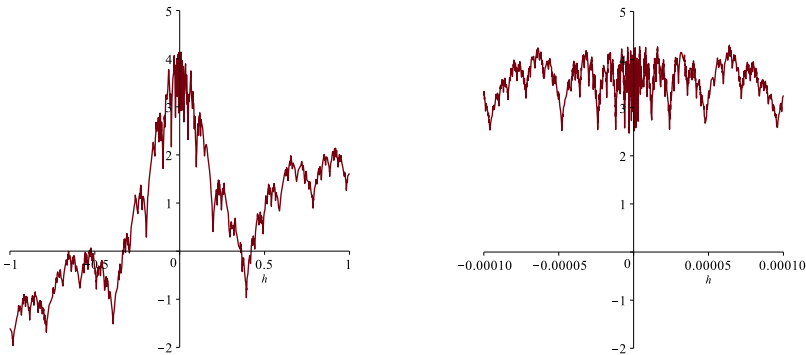


Figure 7. The graph of $(W(3\pi/8) - W(3\pi/8 + h))/\sqrt{|h|}$ for $h \in [-1, 1]$ (left) and for $h \in [-0.0001, 0.0001]$ (right).

We wish to find some integer p so that $2^{-p} \approx |h|$; then we will break the sum into two pieces based on p . The interval $(0, 1]$ can be decomposed into the union of the dyadic intervals $[\frac{1}{2}, 1], [\frac{1}{4}, \frac{1}{2}], [\frac{1}{8}, \frac{1}{4}], \dots$. Since $|h| \in (0, 1)$, we must have that $|h|$ is in one of these dyadic intervals; that is, there exists $p \in \mathbb{N}$ such that $2^{-p} \leq |h| \leq 2^{-p+1}$. Using this p , we split the sum into two pieces and bound each piece:

$$\begin{aligned} |W(t+h) - W(t)| &\leq 2 \sum_{n=0}^{p-1} a^n |\sin(2^{n-1}h)| + 2 \sum_{n=p}^{\infty} a^n |\sin(2^{n-1}h)| \\ &\leq 2 \sum_{n=0}^{p-1} a^n 2^{n-1} |h| + 2 \sum_{n=p}^{\infty} a^n \\ &= |h| \frac{(2a)^p - 1}{2a - 1} + 2 \frac{a^p}{1 - a}, \end{aligned}$$

using the facts that $|\sin(x)| \leq |x|$ and that

$$\sum_{n=0}^{p-1} r^n = \frac{r^p - 1}{r - 1}.$$

Since $2^{-p} \leq |h| \leq 2^{-p+1}$, we have that $2^p |h| \leq 2$ and $a^p = \sqrt{2^{-p}} \leq \sqrt{|h|}$. Thus

$$|W(t+h) - W(t)| \leq \left(\frac{2}{2a-1} + \frac{2}{1-a} \right) a^p \leq \left(\frac{2}{2a-1} + \frac{2}{1-a} \right) \sqrt{|h|} \approx 11.66 \sqrt{|h|}. \quad \square$$

Proof of Theorem 1.2. Set $a = 1/\sqrt{2}$ and $t_{m,k} = m\pi/2^k$ for fixed $m, k \in \mathbb{N}$. Let $0 < |h| \leq 2^{-(k+7)}$. As in the previous proof, we begin by applying the trigonometric identity $\cos(y) - \cos(x) = 2 \sin(\frac{1}{2}x + y) \sin(\frac{1}{2}x - y)$ to obtain

$$W(t_{m,k}) - W(t_{m,k} + h) = 2 \sum_{n=0}^{\infty} a^n \sin(2^n t_{m,k} + 2^{n-1}h) \sin(2^{n-1}h).$$

When $n \geq k+1$, we know $2^n t_{m,k} = 2^{n-k} m\pi$ is a multiple of 2π , and so by the periodicity of the sine function, $\sin(2^n t_{m,k} + 2^{n-1}h) = \sin(2^{n-1}h)$. We split the sum into two pieces, the beginning and the tail:

$$W(t_{m,k}) - W(t_{m,k} + h) = B + T,$$

where

$$B = 2 \sum_{n=0}^k a^n \sin(2^n t_{m,k} + 2^{n-1}h) \sin(2^{n-1}h) \quad \text{and} \quad T = 2 \sum_{n=k+1}^{\infty} a^n \sin^2(2^{n-1}h).$$

We will have established the theorem once we show the two bounds

$$B \geq -0.31\sqrt{|h|} \quad \text{and} \quad T \geq 0.54\sqrt{|h|}. \quad (3-1)$$

We begin by showing the bound on B in (3-1), following similar reasoning to the previous proof:

$$B \geq -2 \sum_{n=0}^k a^n |\sin(2^{n-1}h)| \geq -2 \sum_{n=0}^k a^n 2^{n-1} |h| \geq -|h| \frac{(2a)^{k+1}}{2a-1},$$

since $|\sin(x)| \leq |x|$ and

$$\sum_{n=0}^k r^n = \frac{r^{k+1} - 1}{r - 1}.$$

Recall our assumption that $|h| \leq 2^{-(k+7)}$ and the fact that $2a = \sqrt{2}$. Therefore,

$$B \geq -\sqrt{|h|} \frac{\sqrt{|h|} 2^{(k+1)/2}}{\sqrt{2}-1} \geq -\sqrt{|h|} \frac{2^{-3}}{\sqrt{2}-1} \approx -0.302\sqrt{|h|}.$$

Now we will show the bound on T in (3-1). In proving this, we will assume, without loss of generality, that $h > 0$ (because $\sin^2(-x) = \sin^2(x)$). Since all the terms in T are positive, we can bound the infinite sum below by a partial sum; that is,

$$T = 2 \sum_{n=k+1}^{\infty} a^n \sin^2(2^{n-1}h) \geq 2 \sum_{n=k+1}^p a^n \sin^2(2^{n-1}h),$$

where $p \in \mathbb{N}$ satisfies $2^{-p} \leq h \leq 2^{-p+1}$. To show that this is well-defined, we need to know that $p \geq k+1$. This follows from the assumption that $h \leq 2^{-(k+7)}$, which implies that $2^{-p} \leq 2^{-(k+7)}$ and subsequently $p \geq k+7$.

Our next step is to bound the sine terms. When $0 \leq x \leq 1$, we have $\sin(x) \geq \sin(1) \cdot x$. To apply this to our situation, we need to verify that the argument of the sine terms is in the interval $[0, 1]$: for $n \leq p$ we have that $0 \leq 2^{n-1}h \leq 2^{p-1}h \leq 1$. Therefore

$$T \geq 2 \sum_{n=k+1}^p a^n \sin^2(2^{n-1}h) \geq 2 \sum_{n=k+1}^p a^n (\sin(1) \cdot 2^{n-1}h)^2 = \frac{\sin^2(1)}{2} h^2 \sum_{n=k+1}^p (4a)^n.$$

Set $r = 4a = 2^{3/2}$, and recall that

$$\sum_{n=k+1}^p r^n = \frac{r^{p+1} - r^{k+1}}{r - 1}.$$

Since $h \geq 2^{-p}$,

$$h^2 = h^{3/2} \sqrt{h} \geq (2^{-p})^{3/2} \sqrt{h} = r^{-p} \sqrt{h}.$$

Putting this together, we have

$$\begin{aligned}
 T &\geq \frac{\sin^2(1)}{2} h^2 \sum_{n=k+1}^p (4a)^n \geq \frac{\sin^2(1)}{2} r^{-p} \sqrt{h} \frac{r^{p+1} - r^{k+1}}{r-1} \\
 &= \sqrt{h} \frac{\sin^2(1)}{2} \frac{r - r^{k+1-p}}{r-1} \\
 &\geq \sqrt{h} \frac{\sin^2(1)}{2} \frac{r - r^{-6}}{r-1} \approx 0.547\sqrt{h},
 \end{aligned}$$

where the final inequality follows from $p \geq k + 7$. \square

4. Proof of the phase transition

We bring together the Loewner equation tools discussed in [Section 2](#) and the properties of the Weierstrass function established in [Section 3](#) to prove our main result.

Proof of [Theorem 1.1](#). When $c < \frac{1}{3}$, [Proposition 3.1](#) implies that $cW(t)$ is a $\text{Lip}(\frac{1}{2})$ function with norm below 4. Therefore, [Theorem 2.1](#) ensures that the hull generated by $cW(t)$ is a simple curve in $\mathbb{H} \cup \{cW(0)\}$.

When $c \geq 20$, we will show that the hull generated by $cW(t)$ is not a simple curve in $\mathbb{H} \cup \{cW(0)\}$ by applying [Proposition 2.2](#). To set the stage, let $c \geq 20$, let $k, m \in \mathbb{N}$, let $t_0 = 2^{-k}m\pi - 2^{-(k+7)}$, and define the time-shifted driving function $V(t) = cW(t_0 + t)$. Our proof will be complete once we prove that V captures a real-valued point at or before time $s = 2^{-(k+7)}$, and we will accomplish this by comparing V to a driving function that we understand well.

Let $t \in [0, s]$ and set $h = s - t$. Then by [Theorem 1.2](#),

$$V(s) - V(t) = c(W(2^{-k}m\pi) - W(2^{-k}m\pi - h)) \geq c \cdot 0.2\sqrt{h} \geq 4\sqrt{s-t}.$$

This implies that $V(t) \leq \lambda(t)$ for $\lambda(t) = V(s) - 4\sqrt{s-t}$. Notice also that $V(s) = \lambda(s)$. In other words, V and λ end at the same point, but V is below λ prior to this. Intuitively, this tells us that V must be moving quickly as $t \rightarrow s$, more quickly in fact than the function λ , which we know to capture a real-valued point (by [Lemma 2.3](#)), and so we should expect V will also capture a real-valued point. We simply need to adapt this intuition into a proof. We begin by appealing to [Lemma 2.3](#), which implies that $x(t) = V(s) - 2\sqrt{s-t}$ is a solution (2-1) with driving function λ . Now let $u(t)$ be the solution to (2-1) with driving function V and initial condition $u(0) = x(0)$. We will assume that u is defined on $[0, s]$, because if not, that means that V has captured $u(0)$ before time s and we have nothing left to show.

Assume that $\tau \in [0, s]$ is a time so that $u(\tau) = x(\tau)$. Then since $V(\tau) \leq \lambda(\tau)$,

$$u'(\tau) = \frac{2}{u(\tau) - V(\tau)} \leq \frac{2}{x(\tau) - \lambda(\tau)} = x'(\tau).$$

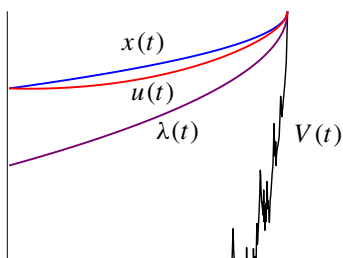


Figure 8. A sketch of the functions $x(t)$, $u(t)$, $\lambda(t)$ and $V(t)$ from the proof of [Theorem 1.1](#).

So at any time when $u(\tau) = x(\tau)$, we have $x(t)$ is increasing more quickly than $u(t)$. This means that $u(t)$ can never pass $x(t)$, and so $u(t) \leq x(t)$ for all $t \in [0, s]$. Note that $u(0) = x(0) = V(s) - 2\sqrt{s} > V(s) - 4\sqrt{s} \geq V(0)$. In other words, $u(t)$ begins to the right of $V(t)$, and so $u(t)$ must remain to the right of $V(t)$ for as long as it is defined. Thus for all $t \in [0, s]$,

$$V(t) \leq u(t) \leq x(t),$$

as illustrated in [Figure 8](#). At time s , we must have $V(s) \leq u(s) \leq x(s) = V(s)$. This implies $V(s) = u(s)$, meaning V has captured the real-valued point $u(0)$ at time s . \square

Acknowledgement

We thank Andrew Starnes for his comments on the first version of the manuscript.

References

- [Gruzberg and Kadanoff 2004] I. A. Gruzberg and L. P. Kadanoff, “The Loewner equation: maps and shapes”, *J. Statist. Phys.* **114**:5–6 (2004), 1183–1198. [MR](#) [Zbl](#)
- [Hardy 1916] G. H. Hardy, “Weierstrass’s non-differentiable function”, *Trans. Amer. Math. Soc.* **17**:3 (1916), 301–325. [MR](#) [JFM](#)
- [Kager et al. 2004] W. Kager, B. Nienhuis, and L. P. Kadanoff, “Exact solutions for Loewner evolutions”, *J. Statist. Phys.* **115**:3–4 (2004), 805–822. [MR](#) [Zbl](#)
- [Lind 2005] J. R. Lind, “A sharp condition for the Loewner equation to generate slits”, *Ann. Acad. Sci. Fenn. Math.* **30**:1 (2005), 143–158. [MR](#) [Zbl](#)
- [Rohde and Schramm 2005] S. Rohde and O. Schramm, “Basic properties of SLE”, *Ann. of Math. (2)* **161**:2 (2005), 883–924. [MR](#) [Zbl](#)
- [Weierstrass 1895] K. Weierstrass, “Über kontinuierliche Functionen eines reellen Arguments, die für keinen Wert des letzteren einen bestimmten Differentialquotient besitzen”, pp. 71–74 in *Mathematische Werke von Karl Weierstrass*, Band 2, Mayer & Müller, Berlin, 1895. [JFM](#)

Received: 2015-09-15

Accepted: 2015-12-13

jlind@utk.edu

Department of Mathematics, University of Tennessee,
Knoxville, TN 37996, United States

jrobins15@gmail.com

University of Tennessee, Knoxville, TN 37996, United States

INVOLVE YOUR STUDENTS IN RESEARCH

Involve showcases and encourages high-quality mathematical research involving students from all academic levels. The editorial board consists of mathematical scientists committed to nurturing student participation in research. Bridging the gap between the extremes of purely undergraduate research journals and mainstream research journals, *Involve* provides a venue to mathematicians wishing to encourage the creative involvement of students.

MANAGING EDITOR

Kenneth S. Berenhaut Wake Forest University, USA

BOARD OF EDITORS

| | | | |
|----------------------|---|------------------------|---|
| Colin Adams | Williams College, USA | Suzanne Lenhart | University of Tennessee, USA |
| John V. Baxley | Wake Forest University, NC, USA | Chi-Kwong Li | College of William and Mary, USA |
| Arthur T. Benjamin | Harvey Mudd College, USA | Robert B. Lund | Clemson University, USA |
| Martin Bohner | Missouri U of Science and Technology, USA | Gaven J. Martin | Massey University, New Zealand |
| Nigel Boston | University of Wisconsin, USA | Mary Meyer | Colorado State University, USA |
| Amarjit S. Budhiraja | U of North Carolina, Chapel Hill, USA | Emil Minchev | Ruse, Bulgaria |
| Pietro Cerone | La Trobe University, Australia | Frank Morgan | Williams College, USA |
| Scott Chapman | Sam Houston State University, USA | Mohammad Sal Moslehian | Ferdowsi University of Mashhad, Iran |
| Joshua N. Cooper | University of South Carolina, USA | Zuhair Nashed | University of Central Florida, USA |
| Jem N. Corcoran | University of Colorado, USA | Ken Ono | Emory University, USA |
| Toka Diagana | Howard University, USA | Timothy E. O'Brien | Loyola University Chicago, USA |
| Michael Dorff | Brigham Young University, USA | Joseph O'Rourke | Smith College, USA |
| Sever S. Dragomir | Victoria University, Australia | Yuval Peres | Microsoft Research, USA |
| Behrouz Emamizadeh | The Petroleum Institute, UAE | Y.-F. S. Pétermann | Université de Genève, Switzerland |
| Joel Foisy | SUNY Potsdam, USA | Robert J. Plemmons | Wake Forest University, USA |
| Erin W. Fulp | Wake Forest University, USA | Carl B. Pomerance | Dartmouth College, USA |
| Joseph Gallian | University of Minnesota Duluth, USA | Vadim Ponomarenko | San Diego State University, USA |
| Stephan R. Garcia | Pomona College, USA | Bjorn Poonen | UC Berkeley, USA |
| Anant Godbole | East Tennessee State University, USA | James Propp | U Mass Lowell, USA |
| Ron Gould | Emory University, USA | József H. Przytycki | George Washington University, USA |
| Andrew Granville | Université Montréal, Canada | Richard Rebarber | University of Nebraska, USA |
| Jerrold Griggs | University of South Carolina, USA | Robert W. Robinson | University of Georgia, USA |
| Sat Gupta | U of North Carolina, Greensboro, USA | Filip Saidak | U of North Carolina, Greensboro, USA |
| Jim Haglund | University of Pennsylvania, USA | James A. Sellers | Penn State University, USA |
| Johnny Henderson | Baylor University, USA | Andrew J. Sterge | Honorary Editor |
| Jim Hoste | Pitzer College, USA | Ann Trenk | Wellesley College, USA |
| Natalia Hritonenko | Prairie View A&M University, USA | Ravi Vakil | Stanford University, USA |
| Glenn H. Hurlbert | Arizona State University, USA | Antonia Vecchio | Consiglio Nazionale delle Ricerche, Italy |
| Charles R. Johnson | College of William and Mary, USA | Ram U. Verma | University of Toledo, USA |
| K. B. Kulasekera | Clemson University, USA | John C. Wierman | Johns Hopkins University, USA |
| Gerry Ladas | University of Rhode Island, USA | Michael E. Zieve | University of Michigan, USA |

PRODUCTION

Silvio Levy, Scientific Editor


Cover: Alex Scorpan

See inside back cover or msp.org/involve for submission instructions. The subscription price for 2017 is US \$175/year for the electronic version, and \$235/year (+\$35, if shipping outside the US) for print and electronic. Subscriptions, requests for back issues from the last three years and changes of subscribers address should be sent to MSP.

Involve (ISSN 1944-4184 electronic, 1944-4176 printed) at Mathematical Sciences Publishers, 798 Evans Hall #3840, c/o University of California, Berkeley, CA 94720-3840, is published continuously online. Periodical rate postage paid at Berkeley, CA 94704, and additional mailing offices.

Involve peer review and production are managed by EditFLOW® from Mathematical Sciences Publishers.

PUBLISHED BY

 **mathematical sciences publishers**
nonprofit scientific publishing

<http://msp.org/>

© 2017 Mathematical Sciences Publishers

involve

2017

vol. 10

no. 1

| | |
|--|-----|
| Intrinsically triple-linked graphs in $\mathbb{R}P^3$ | 1 |
| JARED FEDERMAN, JOEL FOISY, KRISTIN MCNAMARA AND EMILY STARK | |
| A modified wavelet method for identifying transient features in time signals with applications to bean beetle maturation | 21 |
| DAVID MCMORRIS, PAUL PEARSON AND BRIAN YURK | |
| A generalization of the matrix transpose map and its relationship to the twist of the polynomial ring by an automorphism | 43 |
| ANDREW MCGINNIS AND MICHAELA VANCLIFF | |
| Mixing times for the rook's walk via path coupling | 51 |
| CAM MCLEMAN, PETER T. OTTO, JOHN RAHMANI AND MATTHEW SUTTER | |
| The lifting of graphs to 3-uniform hypergraphs and some applications to hypergraph Ramsey theory | 65 |
| MARK BUDDEN, JOSH HILLER, JOSHUA LAMBERT AND CHRIS SANFORD | |
| The multiplicity of solutions for a system of second-order differential equations | 77 |
| OLIVIA BENNETT, DANIEL BRUMLEY, BRITNEY HOPKINS, KRISTI KARBER AND THOMAS MILLIGAN | |
| Factorization of Temperley–Lieb diagrams | 89 |
| DANA C. ERNST, MICHAEL G. HASTINGS AND SARAH K. SALMON | |
| Prime labelings of generalized Petersen graphs | 109 |
| STEVEN A. SCHLUCHTER, JUSTIN Z. SCHROEDER, KATHRYN COKUS, RYAN ELLINGSON, HAYLEY HARRIS, ETHAN RARITY AND THOMAS WILSON | |
| A generalization of Zeckendorf's theorem via circumscribed m -gons | 125 |
| ROBERT DORWARD, PARI L. FORD, EVA FOURAKIS, PAMELA E. HARRIS, STEVEN J. MILLER, EYVINDUR PALSSON AND HANNAH PAUGH | |
| Loewner deformations driven by the Weierstrass function | 151 |
| JOAN LIND AND JESSICA ROBINS | |
| Rank disequilibrium in multiple-criteria evaluation schemes | 165 |
| JONATHAN K. HODGE, FAYE SPRAGUE-WILLIAMS AND JAMIE WOELK | |